On-line spectroscopic study of brominated flame retardant extraction in supercritical CO_2

Dong Xia[a], Ange Maurice[a], Antoine Leybros[b], Jong-Min Lee[a,c], Agnes Grandjean[b] and Jean-Christophe P. Gabriel[a,d*]

[a] *Nanyang Technological University, Energy Research Institute @ NTU (ERI@N), SCARCE Laboratory, 637459, Singapore*.

[b] *CEA, DES, ISEC, DMRC, Univ Montpellier, Marcoule, France*

[c] *Nanyang Technological University, School of Chemical and Biomedical Engineering, 637459, Singapore*.

[d] *Université Paris-Saclay, CEA, CNRS, NIMBE, 91191, Gif-sur-Yvette, France.*

[*]Corresponding author. Jean-Christophe P. Gabriel

E-mail address: Jean-christophe.gabriel@cea.fr / jgabriel@ntu.edu.sg

ABSTRACT

Removal of brominated flame retardants (BFRs) from polymers before disposal or recycling will alleviate negative environmental effects and ensure safe usage of recycled products. Extraction of BFRs in supercritical CO_2 is appealing but also presents challenges to industries due to limited solubility and lack of kinetic studies. For a more comprehensive evaluation of supercritical extraction potentialities, we (i) developed an on-line pressure apparatus that is compatible with both the FTIR and UV-vis spectrometers to enable kinetic and thermodynamic studies; (ii) studied kinetic extraction involving three conventional and two novel BFRs as well as three typical polymeric matrix. Solubilities were determined using the gravimetric method or X-ray fluorescence. FTIR exhibited a superior applicability compared to UV-vis in the following BFR extraction's time-dependency binary and ternary systems. We observed that faster stirring speed, higher temperature, and

finer particle size can accelerate the overall extraction kinetics. In binary systems, it took less than 2 hours to achieve equilibrium for each BFR at 60 °C, 25 MPa and 1000 rpm. In the presence of polymeric matrix, slower extraction kinetics were observed due to the occurrence of competitive dissolution and molecular diffusion within the matrix. Mathematical models derived from irreversible desorption and Fick's diffusion laws fitted well with the observed extraction kinetics of BFRs, thus enabling us to identify the rate-determining step. The high solubilization rate coefficients that we measured for BFRs revealed that the dynamic extraction process in up-scaling design could compensate for the low solubility with flowing supercritical CO_2.

Keywords: Extraction; Kinetic; Brominated Flame Retardant; Spectroscopy; Supercritical CO_2; On-line analysis

1. Introduction

Rapid development in polymer science over the past 60 years has led to the introduction of a tremendous amount of polymeric materials into people's daily life (Hahladakis et al., 2018). To comply with the fire safety standards, the use of flame retardants in various polymeric products is essential. Brominated flame retardants (BFR) are the most effective since they require the lowest amount of material for the highest flame retardancy. Thus, the global market demand for BFRs continues to increase substantially (Birnbaum and Staskal, 2004; Bergman et al., 2012; Gramatica et al., 2016). At present, the market is witnessing a gradual shift in demand for novel BFRs, driven by the phasing-out of widely used BFRs such as polybrominated diphenyl ethers, as a result of the regulations by Stockholm Convention due to concerns over the health risks presented to both the public and the ecosystem (Bramwell et al., 2017; Stubbings et al., 2019). Apart from more than seventy-five types of conventional BFRs, around sixty types of novel BFRs were recently reported to be used world-wide and are ubiquitous in the environment (Georlette, 2001; Liu et al., 2016; Yu et al., 2016; Gill et al., 2020; Zuiderveen et al., 2020).

Indeed, the occurrence of most BFRs in various environmental matrices can cause adverse effects on diverse organisms due to their toxicity (Kim et al., 2014; Xiong et al., 2019). Furthermore, the presence of bromine in BFRs poses many challenges on the proper disposal or recycling of the BFRs. Incineration has the disadvantage of generating corrosive gases and possibly highly toxic PBDD/Fs (Sakai et al., 2001; Ni et al., 2012). Landfilling results in the leaching of toxic brominated substance with possible transfer into local aquifers (Zhou et al., 2013; Cristale et al., 2019). Even in mechanically recycled plastics, uncontrolled BFR additives can cause quality and safety issues. Therefore, the removal of BFRs from polymers has been a necessity in order to recycle or even simply dispose them.

Organic solvent-based extraction has been proposed as a method to remove BFRs from polymers (Nakajima et al., 2002; Altwaiq et al., 2003; Zhang and Zhang, 2012). From the extraction, resulting polymers could be decontaminated and retain most of their original qualities while the used solvents could be recycled by distillation. Hence, some commercial processes have been reported, like CreaSolv, which use a combination of solvents to extract various BFRs (Freegard et al., 2006). Although effective, the use of organic solvents should be minimized due to the related health and safety issues (toxicity, flammability, risks associated with distillation). Moreover, the subsequent distillation and drying processes are energy-intensive, leading to an increase in operational costs. Hydrothermal leaching is also a good alternative to remove bromine and other undesired impurities, but the downside is the cost resulted from effluent treatment (Zhan et al., 2020).

Supercritical CO_2 ($ScCO_2$) presents an attractive advantage over organic solvents for BFR extraction, because it is cheap, non-toxic, non-flammable, has high mass and thermal diffusivity, and also allows for an easy recovery by simple decompression of solvent-free extracted substances (Taylor, 1996; Kayathi et al., 2020). Solubility is important to determine the theoretical limits of extractability, thus, solubilities of some conventional BFRs have been measured in $ScCO_2$ as function of pressure and temperature (Gamse et al., 2000;

64 Peng et al., 2014). Also, $ScCO_2$ extraction of BFRs has been proven to be of varying degrees of success in terms
65 of the extraction efficiency with or without co-solvents (Marioth et al., 1996; Suzuki et al., 2002; Altwaiq et al.,
66 2003). Nevertheless, challenges from the investigation of extraction kinetics to validate process scale-up and
67 develop successful industrial processes remained (Nimet et al., 2011; Sodeifian et al., 2016; Villanueva-Bermejo
68 et al., 2020). To our knowledge, there have only been few of such studies reported previously, either off-line or
69 on-line, for BFR extraction (Bunte et al., 1996; Wang et al., 2004). This study proposes to evaluate feasibility of
70 BFR extraction in $ScCO_2$ considering thermodynamic and kinetic point of view. The spectroscopic technique
71 allows for on-line and non-invasive monitoring of concentration in supercritical conditions (Laintz et al., 1991;
72 Carrott and Wai, 1998; Wang et al., 2004; Wang et al., 2018). Therefore, we report a method coupling versatile
73 high pressure vessel with both UV-vis and mid-IR spectrometers and demonstrate their applicability: (i) to
74 perform spectroscopic analysis of multi-component mixtures such binary, ternary, and even more complexed
75 mixtures in $ScCO_2$ media; and (ii) to investigate the effects of temperature, pressure, stirring, and particle size
76 and type of polymeric matrix on extraction kinetics for various BFRs.

77 **2. Materials and methods**

78 2.1 Materials

79 BFR compounds: (i) 3,3',5,5'-Tetrabromobisphenol A (TBBPA) and (ii) 1,2,5,6,9,10-
80 Hexabromocyclododecane (HBCD or HBCDD) were purchased from Sigma-Aldrich (St. Louis, MO, USA); (iii)
81 Decabromodiphenyl ether (DBDBE or BDBE 209) and (iv) 2,4,6-Tris(2,4,6-tribromophenoxy)-1,3,5-triazine
82 (TTBP-TAZ) were purchased from Macklin (Shanghai, China); (v) 2,2-Bis[3,5-dibromo-4-(2,3-
83 dibromopropoxy)phenyl]propane (TBBPA-BDBPE) was purchased from Aladdin (Shanghai, China). The five
84 selected BFR compounds include three of the most commonly used conventional BFRs and two of the most

85 popular novel ones (Alaee, 2003; Covaci et al., 2011; Ma et al., 2016; Lörchner et al., 2019). Chemical
86 structures and detailed information of the five BFRs are presented in Fig. S. 1 and table S. 1, respectively. Since
87 HBCD and DBDBE have relatively lower purities, they were purified in flowing $ScCO_2$ at 60 °C and 25 MPa for 6
88 h (Gamse et al., 2000). Other BFR compounds were used without any further purification.
89 Ultra-pure water was obtained from a water purification system (WaterPro®, Labconco Co., USA), with a
90 resistivity of 18.2 MΩ·cm at 25 °C.
91 Liquid CO_2 was supplied by CryoExpress Pte. Ltd. (Singapore) with a purity of 99.9%.
92 Acrylonitrile butadiene styrene (ABS), polystyrene (PS) and high-impact polystyrene (HIPS) resins were
93 selected as typical polymer substrates for additive BFRs because they are commonly used in consumer products
94 and construction materials where BFRs are applied. BFR-containing ABS pellets were fabricated following the
95 industrial practices using hot blending and extrusion with an additive proportion of 13-14 wt.% of TBBPA or
96 TBBPA-BDBPE (Shandong Tianyi Chemical Co.,China). TBBPA-containing PS and HIPS pellets (13-14 wt.%
97 of TBBPA) were prepared by mixing virgin resin and TBBPA in tetrahydrofuran solution (THF, ACS reagent,
98 Sigma-Aldrich, USA), and by subsequent solvent evaporation. We then grinded these as-obtained pellets into
99 powders with a centrifugal mill (ZM 200, Retsch, Germany), at cryogenic temperature using liquid N_2, then
100 sieved the powders into two particle size fractions (D_{ABS}) in the ranges: (i) 0.25-1 mm, and (ii) less than 0.25
101 mm.
102 2.2 Experimental apparatus
103 A schematic representation of our $ScCO_2$ extraction system optically coupled with on-line spectrometers
104 (FTIR and UV-vis) is shown in Fig. 1. The extraction reactor, which is a core part of the system, is a commercial
105 pressure vessel from Parr Instrumental Company, USA (ref. 2430HC2). It was modified according to our
106 requirements with the optical windows to enable spectroscopic studies for operating pressure and temperature

ranging up to 35 MPa and 200 °C. The vessel has an entire volume of 75.4 mL, with minimized dead volumes from filling and venting ports. Two dismountable windows (made of sapphire for FTIR or fused silica for UV-vis; rupture modulus: 1200 MPa versus 100 MPa; diameter: 25 mm; thickness: 15.7 mm) are located on each side of the vessel in opposition to each other. Each window is kept in place with the presence of a window holder and sealed by two Teflon sealants through "opposed force" (Fig. S. 2). The resulted optical path length is measured to be 58 mm, which is sufficiently long to give good sensitivity (>0.001 mM) and limits of detection (Jackson et al., 1995; Poliakoff et al., 1995).

For the other parts of the $ScCO_2$ extraction system (Fig. 1a), liquid CO_2 is first cooled by a circulation chiller (F250, Julabo, Germany) prior to its delivery to a dual piston pump (LD-Class, Teledyne ISCO, USA). The vessel temperature is monitored using a K-type thermocouple inserted into a stainless steel plunger. Two PID controlled (E5CC, Omron, Japan) electric cartridge heaters, slid into the cavities at the bottom of the vessel, are used to raise the vessel's temperature. A magnetic agitator (MR 3001 K, Heidolph, Germany) drives a 12×3 mm Teflon-coated stirring bar to stir the contents in the vessel. The additional accessories permit measurements of pressure, temperature, and agitation speed with a precision of 0.1 MPa, 0.1°C, and 3%, respectively.

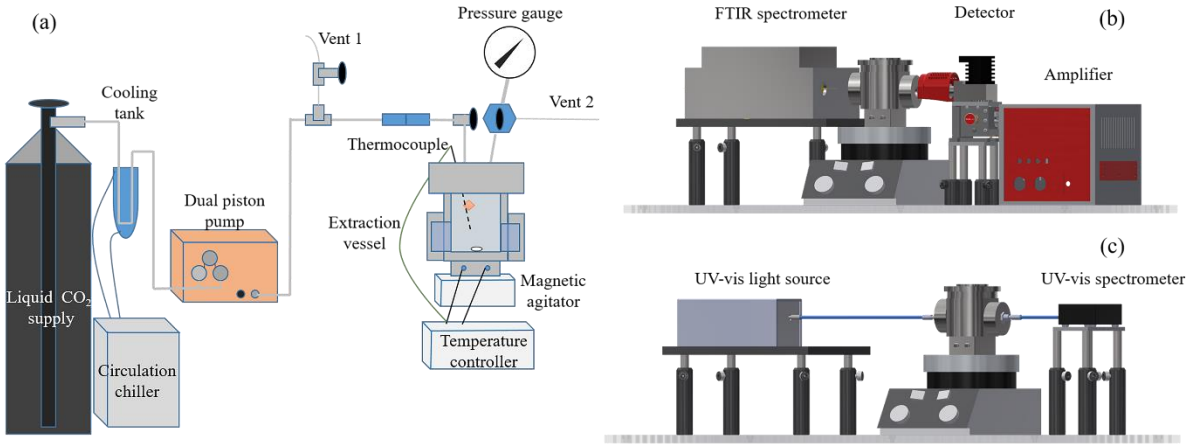

Fig. 1. Schematic illustration of the experimental $ScCO_2$ extraction system (a), where each component of the system is not presented in proportion; the virtual deployment of the vessel with FTIR (b) and with UV-vis spectroscopic components (c),

where the vessel head parts (model 4792) and the spilt rings (A455HC) are abridged for clearly presenting their optical alignment.

The spectroscopic components are combined with the $ScCO_2$ extraction system in a modular fashion (Fig. 1b and Fig. 1c). Their optical alignment can be readily adjusted with the bases and supporting rods purchased from Thorlabs Inc. (USA). The IR beam provided by a FTIR spectrometer (Bruker Alpha OEM, Bruker Optics Inc., Germany) transmits through the vessel, and the signals are detected by a Stirling Cycle Cooled detector that is connected with an amplifier (K508-MCT1000, Infrared Associates, USA) (C. Penisson, 2018; Kokoric et al., 2018; Maurice et al., 2020).

For UV-vis monitoring, the UV radiation emanating from a deuterium light source (DH-MINI, Ocean Optics Inc., UK) is transferred through the vessel, a pair of optical fibers, and several collimating lenses. Spectra were recorded by a UV-vis spectrometer (Flame-T, Ocean Optics Inc., UK).

2.3 Measurement of extraction kinetics

Prior to each extraction, a thorough clean-up of the $ScCO_2$ extraction system was performed with flowing $ScCO_2$ until the baseline absorbance was constant, and then the reference spectra of pure $ScCO_2$ were recorded using identical operating conditions for sample spectra. To assess reproducibility, each extraction was performed in triplicate. Accurately weighted pure BFR powders (100 mg) or polymer powders (600 mg) were enclosed within Solidweave mesh (Mesh size=9 μm) package, which was then attached inside the vessel, close to the filling port. After loading the sample, the vessel was hermetically closed and then flushed three times with gaseous CO_2. Then it typically took around 10 minutes to reach the desired temperature and pressure, prior to stirring at a set speed. Spectra were collected at regular intervals during the whole extraction process. IR spectra were collected with a 4 cm^{-1} resolution and were obtained by the Fourier transformation of 64 interferograms. UV spectra were averaged from 1000 scans within an integration time of 0.015 s. Each extraction experiment

was terminated after reaching a steady state condition where spectra no longer show any change in absorbance. The following decompression procedure was fast (less than 10 s) followed by subsequent refilling with gaseous CO_2 and no re-deposition of solute back to sample mesh could be observed under a microscope (×500, RS Pro).

2.4 Determination of saturated concentration

Solubility, expressed as saturated concentration (c_s, in mM), is the maximum concentration of a solute that can be dissolved in a solvent. c_s of individual pure BFR in $ScCO_2$ was measured gravimetrically using an analytical balance (MS105, Mettler-Toledo, USA) with a readability of 0.01 mg and calculated with the following equation:

$$c_s = 10^3 \cdot (m_2 - m_1)/[M_{BFR} \cdot (V_v - V_s)] \quad (1)$$

where m_1 and m_2 indicate the weight of polymer sample before and after extraction; M_{BFR} denotes the molar mass of the BFR molecule. V_v is the vessel volume and V_s is the sample package volume determined with the water discharging method.

Since mass removal of BFR is not gravimetrically measurable in polymer samples, the Br content of polymer samples ($C_{Br/polymer}$, in wt.%) before and after extraction were determined using an X-ray fluorescence analyzer (XRF) (Vanta C, Olympus, Japan) applying RoHS plus method. For this determination, the powdered polymer samples (200 mg) were pressed into a circular shaped disc using a hydraulic crimper (MSK-510M, MTI Co., China) at 160 °C and 5 MPa for 5 min. The mass removal of BFR in polymer matrix was calculated using the formula $\Delta(C_{Br/polymer} \cdot m)/C_{Br/BFR}$, where $C_{Br/BFR}$ is Br content in BFR compound (wt.%), only then the solubility can be calculated with Eq. (1) .All experimental data were displayed in a format of mean value ± standard deviation.

2.5 IR spectroscopy and data processing

The IR spectra were processed with a software combination of OPUS 7.5 and Python 3.6.8. After baseline

correction, the corresponding absorbance peak of interest (A) (Table S. 2) was integrated in the wavenumber region of w_2-w_1 (in cm^{-1}) using the following equation:

$$A = \int_{w_1}^{w_2} \log_{10}\left(\frac{I_0}{I_t}\right) dw \quad (2)$$

with I_0 and I as sample and baseline intensity, respectively.

According to Beer-Lambert Law, the integrated absorbance was proportionally converted to BFR concentration (c, in mmol/L) in $ScCO_2$ (IUPAC, 1997): $c_t = A_t \cdot c_s / A_s$, where the subscripts t and s indicate timely and saturation readings.

Furthermore, the linear sum of the absorbance spectra of each component (A_i) was considered for quantitative interpretation of the overlapped peak area of a mixture (A_m):

$$A_m = \sum_{i=1}^{N} A_i \quad (3)$$

2.6 Mathematical modelling of extraction kinetics

In the outline, the $ScCO_2$ extraction of compounds from solid matrices (porous or not) can be condensed into a four-step process: (i) diffusion of $ScCO_2$ into the internal structure of solid matrices; (ii) desorption and solvation of solute in $ScCO_2$; (iii) intra-particle diffusion of the mixture of solute and $ScCO_2$ to the solid interface; and (iv) diffusion of the mixture from the solid interface to the bulk $ScCO_2$ (Madras et al., 1994; Sunarso and Ismadji, 2009; Huang et al., 2012). All these steps are diffusion limiting steps except for the solubilization step (ii).

To achieve specific description of extraction kinetics involving complex phenomena with mathematical models, we introduced two simplified scenarios, including the absence of matrix and well stirred reactor, based on the assumption that the diffusion steps can be controlled by changing of matrix properties or stirring speed. Hence, the basic physicochemical models can be applied (Srinivasan et al., 1990). For the solubilization step, an irreversible and first order model (linear desorption) was applied to calculate the solubilization rate coefficient (k_S,

190 in h^{-1}) over the extraction period (t, in h). The equation can be expressed in an integrated form (Tan and Liou,

191 1989; Elektorowicz et al., 2007; Jokić et al., 2010):

192 $$\ln[(c_s - c_t)/c_s] = -k_S \cdot t \quad (4)$$

193 The model for the diffusion steps is based on a hot sphere diffusion model derived from Fick's diffusion

194 laws assuming that the loaded particles consist of solid spheres with uniform radius and initial concentration of

195 extracted substance and are immersed into a fluid free from the substance (Crank, 1979; Bartle et al., 1990; Huang

196 et al., 2012). The model is expressed as:

197 $$\frac{c_t}{c_s} = 1 - \frac{6}{\pi^2}\sum_{n=1}^{\infty}\frac{1}{n^2} \cdot \exp\left[-\left(\frac{n\pi}{R}\right)^2 D_e t\right] \quad (5)$$

198 with D_e as effective diffusion coefficient in a solid substrate ($m^2 \cdot h^{-1}$) and R as radius of spherical solid particles

199 (m). For long time, all terms except the first in the series of exponential terms in Eq. (5) become negligible and

200 the kinetic curve can be rewritten as:

201 $$\ln[(c_s - c_t)/c_s] = \ln\left(\frac{6}{\pi^2}\right) - \frac{\pi^2 D_e}{R^2} \cdot t \quad (6)$$

202 where $\pi^2 D_e/R^2$ may also be recast as diffusion rate coefficient k_D (h^{-1}).

203 From Eq. (4) and Eq. (6), a plot of $\ln[(c_s\text{-}c_t)/c_s]$ versus t may fall onto two intersecting straight lines with

204 different slops k_1 and k_2 (Subra et al., 1998; Hojnik et al., 2008).

205 In addition, absolute average relative deviation (AARD, %) between the experimental data ($c_{t,exp}$) and the

206 modeled data ($c_{t,mod}$) is also evaluated by:

207 $$\text{AARD} = \frac{100}{N}\sum_{i=1}^{N}\frac{|c_{t,exp} - c_{t,mod}|}{c_{t,exp}} \quad (7)$$

208 **3. Results and discussion**

209 3.1 Comparison between FTIR and UV-vis spectroscopies

210 In this study, FTIR and UV-vis spectroscopies were first compared for their applicability to characterize

211 BFR compounds in $ScCO_2$. Raman spectroscopy was not suitable because it suffers from a lack of sensitivity
212 when solute concentrations are low (Jackson et al., 1995). In terms of spectrum window, the FTIR reference
213 spectrum was narrowed to two available bands of 4500-3880 cm^{-1} and of 3500-2600 cm^{-1} (Fig. S. 3a). The other
214 IR bands, including the fingerprint C-Br group (690-515 cm^{-1}), were completely obscured by the absorptions of
215 the sapphire windows and $ScCO_2$ itself (Poliakoff et al., 1995). To circumvent this problem, some identifiable
216 groups, like ν (C-H) and ν (O-H), were employed to characterize BFRs in $ScCO_2$ (Table S. 2). However, due to
217 the ubiquity of these groups in organic chemicals, the high purity of BFR compounds and the cleanliness of
218 reference spectra must be ensured to characterize BFRs in $ScCO_2$, especially for a quantitative purpose.
219 Comparatively, the spectral window of UV-vis could extend to almost the whole spectrometer's range (200-800
220 nm) (Fig. S. 3b).
221 With well-defined reference spectra, TBBPA, the most commercially used BFR, was characterized as an
222 example in $ScCO_2$ using FTIR and UV-vis spectrometers (Fig. 2). Both spectra demonstrated incremental
223 absorbance with extraction time until they leveled off and reached a stable value. The FTIR spectrum of TBBPA
224 was marked by two bands, with two maximum absorbance located at 2904 cm^{-1} and 3000 cm^{-1}, resulting from ν
225 (C-H alkane) and composite ν (C-H combinations) absorption, respectively (Fulton et al., 1993). In the UV-vis
226 spectrum, TBBPA showed two absorption bands (200-260 nm and 260-310 nm) as a result of electronic
227 transitions, $\pi \rightarrow \pi^*$ transition of conjugated C=C group (Lu et al., 1999; Khaled et al., 2018). However, there was
228 an absorbance saturation problem in the UV-vis spectrum of TBBPA. This was due to the high absorptivity of
229 the chromophore in the UV region. Moreover, a shift of peaks in the UV-vis spectra was apparent with the
230 increase of concentration, which resulted in an ambiguous peaks' interpretation.

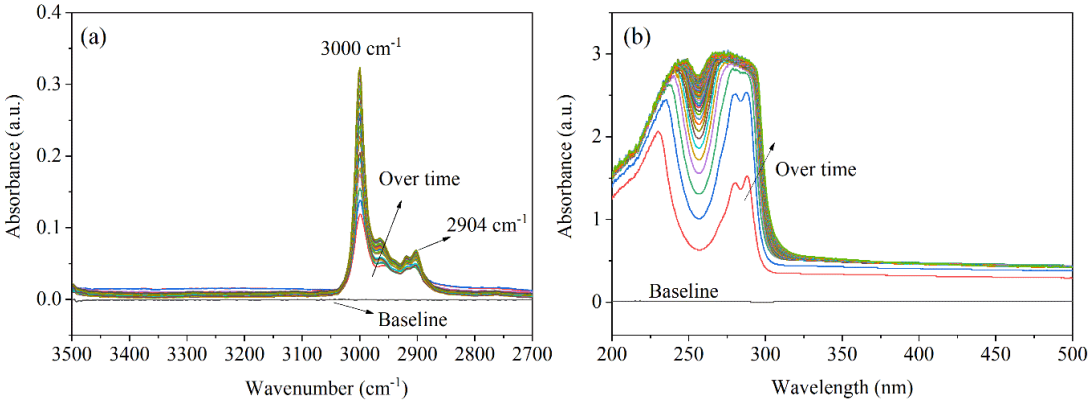

Fig. 2 FTIR (a) and UV-vis (b) spectra of TBBPA in $ScCO_2$ over extraction period at 60°C, 20 MPa, and 1000 rpm.

Although each of the technique has its own advantages and shortcomings from the spectroscopic standpoint, FTIR is a better technique than UV-Vis for carrying out the on-line monitoring. In addition, sapphire has higher rupture modulus as compared to fused silica. This will allow for a safer operating condition under high pressure. Therefore, only FTIR spectroscopy was used in the following sections.

3.2 Effect of operating conditions

To study the influence of operating conditions on the extraction performance of BFR in $ScCO_2$, BFR+$ScCO_2$ binary systems were first explored based on a simplified scenario where the matrix was absent, thus the matrix related diffusion steps (i) and (iii) might be negligible (see section 2.6). Regarding the binary equilibria of TBBPA and $ScCO_2$, the list of operating conditions explored and the fitting parameters are given in Table 1 and the corresponding kinetic curves are illustrated in Fig. 3. The c_s value of TBBPA at 60 °C, 20 MPa and 0 rpm was previously reported of 0.363 mM (Gamse et al., 2000), which is in good agreement with our results, thus allowing us to validate our apparatus for c_s measurement. All the kinetic curves showed similar trend where the concentration of TBBPA approached its asymptotic value gradually after an initial rapid increase.

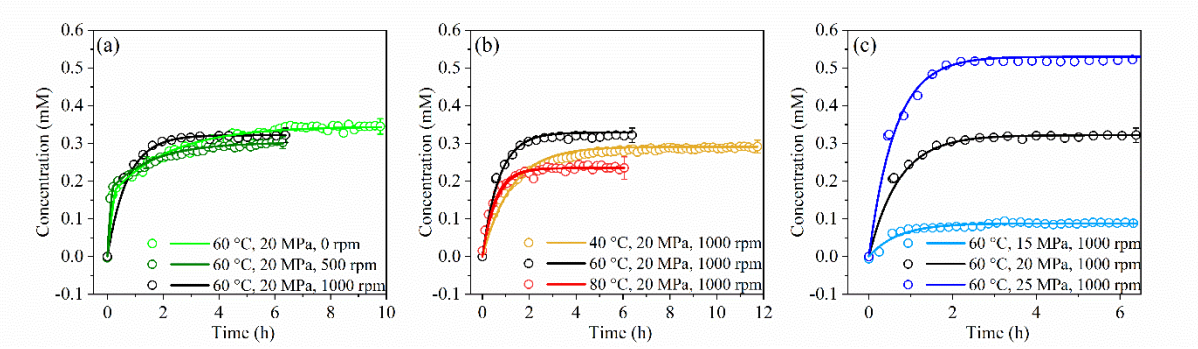

247

248 Fig. 3 Influence of operating conditions on $ScCO_2$ kinetic extraction of TBBPA: stirring speed (a), temperature (b), and

249 pressure (c). Discrete points and solid lines denote experimental and fitted results, respectively.

250 Table 1 Solubilities and kinetic parameters of selected BFRs in binary system.

BFRs	Operating conditions	c_s	k_S	AARD
		mM	h^{-1}	%
TBBPA	40 °C, 20 MPa, 1000 rpm	0.291±0.004	0.81±0.04	3.16
	60 °C, 15 MPa, 1000 rpm	0.088±0.004	1.43±0.19	4.14
	60 °C, 20 MPa, 0 rpm	0.345±0.026	0.48±0.03	2.52
	60 °C, 20 MPa, 500 rpm	0.302±0.016	0.66±0.04	2.28
	60 °C, 20 MPa, 1000 rpm	0.322±0.019	1.40±0.04	1.11
	60 °C, 25 MPa, 1000 rpm	0.531±0.014	1.59±0.08	2.22
	80 °C, 20 MPa, 1000 rpm	0.235±0.007	1.84±0.09	3.70
HBCD	60 °C, 25 MPa, 1000 rpm	0.064±0.004	4.68±1.09	4.22
DBDPE	60 °C, 25 MPa, 1000 rpm	0.004±0.000	N.C.	N.C.
TBBPA-BDBPE	60 °C, 25 MPa, 1000 rpm	0.154±0.002	4.68±0.91	5.70
TTBP-TAZ	60 °C, 25 MPa, 1000 rpm	0.012±0.001	8.10±1.06	3.71

251 N.C. means not calculated.

Stirring was found to be able to improve the extraction kinetics and shorten the time required to achieve saturation from 6 hours to 2 hours, without significantly changing the solubility when comparing the three cases of non-stirring (0 rpm), 500 rpm, and 1000 rpm (Fig. 3a). We observed that the overall experimental scatterplots fitted well with the first order kinetic equation only at the highest stirring speed. This indicates that the external diffusion step can be negligible in the well stirred reactor (the second simplified scenario, see section 2.6) by fast stirring, thus leading to a solubilization-dominated process. We conclude that the external diffusion becomes more significant with less powerful stirring. Since the rapid increase of concentration during the initial compression period was largely due to the inevitable agitation caused by filling turbulences, the fitting model was only applied after the initial compression period in the 0 rpm and 500 rpm cases, where the decreased k_S should be attributed to external diffusion.

The effects of temperature and pressure on the extraction of TBBPA were explored at a constant stirring speed of 1000 rpm (Fig. 3b and Fig. 3c). The increase in the k_S value was more than double with the increase in temperature from 40 °C to 80 °C, while the highest c_s occurred at the intermediate temperature of 60 °C for the studied pressure. Furthermore, temperature-dependent rate coefficients comply well with Arrhenius equation, which states that the natural logarithm of rate coefficient is proportional to the inverse of absolute temperature (Connors, 1990). However, the k_S value was barely affected by the pressure increase from 15 to 25 MPa at 60 °C, although the solubility was significantly improved.

In consideration of both the kinetic and thermodynamic aspects, an optimized operating condition (60 °C, 25 MPa, 1000 rpm) was also applied for the other four BFRs. As shown in Fig. 4, each BFR had a characteristic spectrum within the band of 3800-2700 cm^{-1}, resulting in a kinetic curve except for DBDBE, which does not contain any identifiable groups in its chemical structure. The characteristic spectral patterns were also verified by additional ATR-FTIR characterization of pure BFR powders (Fig. S. 4). In the actual comparison with ATR-

FTIR spectra, the on-line FTIR spectra showed a general red shift due to the formation of hydrogen bonding in $ScCO_2$ (Fulton et al., 1993; Poliakoff et al., 1995). Moreover, the relative absorbance intensity for different groups varied in the FTIR spectra, possibly due to the existence of $ScCO_2$ and sapphire windows. For HBCD, TBBPA-BDBPE, and TTBP-TAZ, their solubilities in $ScCO_2$ were lower than that of TBBPA but the duration required to reach equilibria were all less than one hour. DBDBE had the lowest solubility, hence it was identified as the most difficult BFR to extract (Peng et al., 2014). Overall, high rate coefficients indicate that a dynamic extraction with flowing $ScCO_2$ could be a more efficient process, because the concentration gradient can be kept high enough to drive BFRs extraction despite their low solubilities.

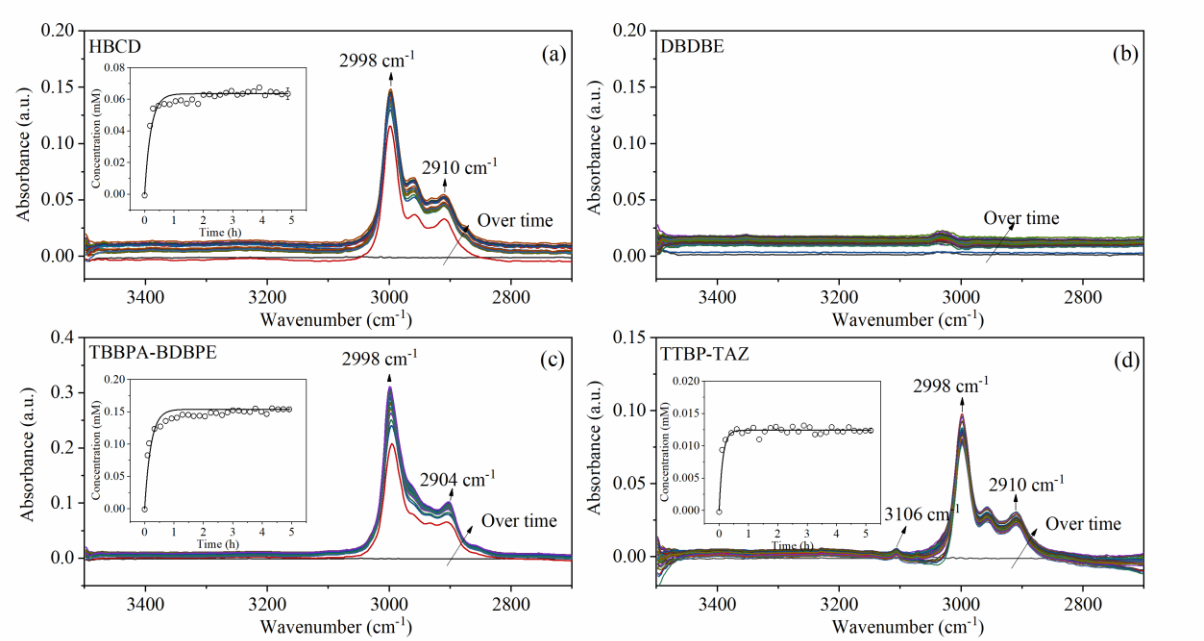

Fig. 4 FTIR spectra over extraction period and resulted kinetic curves of BFRs at 60 °C, 25 MPa, and 1000 rpm.

3.3 Effect of loading water as cosolvent

In ternary systems, water was first included as a co-solvent along with BFR and $ScCO_2$ since a small amount of water added to $ScCO_2$ was reported to be able to increase the solubility of polar species in non-polar solvent (Jackson et al., 1995). The FTIR spectra of TBBPA with loading of ultra-pure water (200 μL, below saturation) were recorded over the extraction period (Fig. S. 5a). The absorbance caused by O-H stretching of

289 H_2O molecules did not interfere with the absorbance of TBBPA, thus the kinetic curve for both TBBPA and H_2O

290 can be followed simultaneously (Fig. S. 5b). Despite an improved c_s of TBBPA by 7% in the presence of such

291 small amount of water, its k_S decreased by 43% possibly due to competitive association between TBBPA and

292 H_2O molecules with $ScCO_2$ (Table 1 and Table 2). Thus, an optimum of extraction performance in the presence

293 of water has to be included in future research. Herein, FTIR spectroscopy provides another advantage over UV-

294 vis spectroscopy because water lack spectral transitions in the UV region.

295 Table 2 Solubilities and kinetic parameters of selected BFRs in ternary systems and more complexed systems at 60 °C, 25

296 MPa, 1000 rpm.

BFRs	Cosolvent or matrix effect	c_s	k_S	k_D	D_e	AARD
		mM	h^{-1}	h^{-1}	$m^2 \cdot h^{-1}$	%
BFR+H_2O+$ScCO_2$						
TBBPA	Loading of 200 μL H_2O	0.570±0.007	0.91±0.05	N.C.	N.C.	3.59
BFR/Polymer+$ScCO_2$						
TBBPA	ABS, D_{ABS} <0.25 mm	0.385±0.001	1.78±0.08	1.08±0.05	$<1.7\times10^{-9}$	2.04
TBBPA	ABS, D_{ABS} 0.25-1 mm	0.376±0.003	0.49±0.08	0.25±0.02	4.0×10^{-10}-6.3×10^{-9}	1.95
TBBPA-BDBPE	ABS, D_{ABS} <0.25 mm	0.149±0.001	1.94±0.37	1.32±0.08	$<2.1\times10^{-9}$	2.88
TBBPA	PS, D_{ABS} <0.25 mm, residue THF	1.216±0.104	N.C.	N.C.	N.C.	N.C.
TBBPA	HIPS, D_{ABS} <0.25 mm, residue THF	0.701±0.008	N.C.	N.C.	N.C.	N.C.

297 N.C. means not calculated.

298 3.4 Effect of polymeric matrix

299 To discover the matrix effect on the extraction performance, BFR-free resins (ABS, PS, and HIPS) were

used as polymeric substrate for incorporation with the BFRs, including TBBPA and TBBPA-BDBPE. The FTIR spectra of each extraction experiment are presented in Fig. S. 6 and Fig. S. 7. The extraction of resins can also be observed, indicating that $ScCO_2$ has a certain degree of solvation power on the polymeric resins, which can increase with temperature and pressure, thus leading to the undesirable dissolution of monomers or oligomers into $ScCO_2$ (Sikorski, 1993; Zhao et al., 2018). In the case of TBBPA-containing ABS samples, the effect of particle size on their extraction performance was investigated, as shown in Fig. 5. We observed faster extraction process with finer particle size. The kinetic curves can be decomposed in two phases, where the first rapid extraction is followed by a slower one. The c_s of TBBPA were of similar value, 0.33 mM, lower than that of the extraction without ABS matrix (0.53 mM) due to the competitive dissolution of ABS polymers.

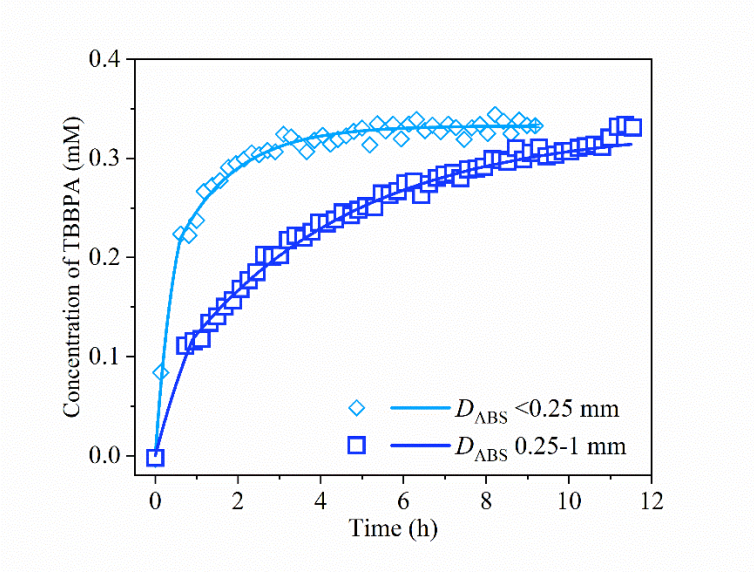

Fig. 5 Effect of polymer particle size on extraction of TBBPA incorporated ABS samples in $ScCO_2$ at 60 °C, 25 MPa, 1000 rpm.

According to the broken and intact cell concept, analytes can be distributed at the outer surface of particles and embedded into their inner structure. This is similar to the BFR-containing ABS powders after grinding, resulting in easily accessible BFRs and less accessible BFRs, respectively (Sovová, 1994). Hence, the first rapid extraction of the so-called washing process was controlled by solubilization in the well stirred reactor and k_1 can be assigned to k_S (Table 2). Furthermore, the sudden reduction of extraction rate after the first part indicates the

completion of accessible BFR's extraction and the intra-particle diffusion resistance came into the effect (Srinivasan et al., 1990; Alexandrou et al., 1992; Grosso et al., 2010). The k_D value can be calculated by $k_D=k_1-k_2$ and D_e range can also be estimated according to Eq. (6). The samples containing TBBPA-BDBPE also supported the two-stage extraction process and the applied models provided very good approximation of the experimental data with AARD lower than 2.9%.

Since TBBPA-incorporated PS and HIPS samples inevitably contained THF residue trapped in the polymer matrix, and THF had high miscibility in $ScCO_2$, the additional absorbance caused by THF with unknown amount was hard to quantify in the studied band. Therefore, we only demonstrated the solubility of TBBPA in Table 2 and the bulk extraction kinetics of aromatic compounds, from TBBPA and the resin matrix, without modelling (Fig. S. 8). The results also showed that it took around 4 hours to reach the equilibria for PS and HIPS samples, similar to the ABS sample with identical particle size. Thus, this indicates that the polymeric type may not affect the extraction rate. However, the inclusion of THF as cosolvent significantly increased the solubility of TBBPA.

4. Conclusions

In this study, a supercritical reactor was assembled with on-line spectroscopic components to study the BFR extraction in $ScCO_2$. A notable feature of the apparatus that can be applicable beyond the current study, is the compatibility with both UV-vis and FTIR spectrometer using the same vessel, enabling the researchers to acquire more comprehensive spectral information of multi-component mixtures in real time and follow their kinetic studies. For quantitative characterization of the BFRs in $ScCO_2$, FTIR spectroscopy is preferred over the UV-vis due to its proper detection range and clearer spectral interpretation despite its limited spectral window. Five BFR molecules were studied using the on-line FTIR technique along with mathematical modelling. Sufficiently fast stirring could eliminate limitations due to the diffusion of molecules in $ScCO_2$, and both higher

temperature and finer grinding size could also accelerate extraction kinetics. However, the pressure and the type of polymer matrix do not significantly affect the extraction kinetics in the considered range. High extraction rates could compensate for low solubility if one applies a dynamic extraction with flowing $ScCO_2$. Overall, extraction parameters provided here are valuable to enable a scale-up process design.

CRediT authorship contribution statement

Dong Xia: Methodology, Investigation, Formal analysis, Writing - original draft. **Ange Maurice**: Software. **Antoine Leybros**: Methodology, Writing - review & editing. **Jong-Min Lee**: Resources. **Agnes Grandjean**: Formal analysis, Writing - Review & Editing. **Jean-Christophe P. Gabriel**: Conceptualization, Methodology, Writing - review & editing, Supervision, Project administration.

Acknowledgments

We acknowledge intern Li-Yi Ang for her assistance in experimental investigation during her Final Year Project in Nanyang Technological University. JCG acknowledge the Region Pays de la Loire for "Young Researcher" funding for the purchase of Parr $ScCO_2$ core reactor (1999). All authors acknowledge financial support from SCARCE laboratory. SCARCE is supported by the National Research Foundation, Prime Minister's Office, Singapore, the Ministry of National Development, Singapore, and National Environment Agency, Ministry of the Environment and Water Resource, Singapore under the Closing the Waste Loop R&D Initiative as part of the Urban Solutions & Sustainability - Integration Fund (Award No. USS-IF-2018-4).

Reference

Alaee, M., 2003. An overview of commercially used brominated flame retardants, their applications, their use

patterns in different countries/regions and possible modes of release. Environ. Int. 29, 683-689. https://doi.org/10.1016/S0160-4120(03)00121-1.

Alexandrou, N., Lawrence, M.J., Pawliszyn, J., 1992. Cleanup of complex organic mixtures using supercritical fluids and selective adsorbents. Anal. Chem. 64, 301-311. https://doi.org/10.1021/ac00027a011.

Altwaiq, A.m., Wolf, M., van Eldik, R., 2003. Extraction of brominated flame retardants from polymeric waste material using different solvents and supercritical carbon dioxide. Anal. Chim. Acta 491, 111-123. https://doi.org/10.1016/S0003-2670(03)00785-2.

Bartle, K.D., Clifford, A.A., Hawthorne, S.B., Langenfeld, J.J., Miller, D.J., Robinson, R., 1990. A model for dynamic extraction using a supercritical fluid. J. Supecrit. Fluids 3, 143-149. https://doi.org/10.1016/0896-8446(90)90039-O.

Bergman, Å., Rydén, A., Law, R.J., de Boer, J., Covaci, A., Alaee, M., Birnbaum, L., Petreas, M., Rose, M., Sakai, S., 2012. A novel abbreviation standard for organobromine, organochlorine and organophosphorus flame retardants and some characteristics of the chemicals. Environ. Int. 49, 57-82. https://doi.org/10.1016/j.envint.2012.08.003.

Birnbaum, L.S., Staskal, D.F., 2004. Brominated flame retardants: cause for concern? Environ. Health Perspect. 112, 9-17. https://doi.org/10.1289/ehp.6559.

Bramwell, L., Harrad, S., Abdallah, M.A.-E., Rauert, C., Rose, M., Fernandes, A., Pless-Mulloli, T., 2017. Predictors of human PBDE body burdens for a UK cohort. Chemosphere 189, 186-197. https://doi.org/10.1016/j.chemosphere.2017.08.062.

Bunte, G., Haerdle, T., Krause, H., Marioth, E., 1996. Extraction of brominated flame retardents with supercritical CO2. Process Technology Proceedings. Elsevier, pp. 535-539. https://doi.org/10.1016/S0921-8610(96)80093-8.

C. Penisson, A.W., J. Theisen, V. Kokoric, B. Mizaikoff, J.C.P. Gabriel, 2018. Water activity measurement of NaCl/H2O mixtures via substrate-integrated hollow waveguide infrared spectroscopy with integrated microfluidics. Nanotech 2018. CRC Press, Anaheim, CA, USA, pp. 198-201.

Carrott, M., Wai, C., 1998. UV− visible spectroscopic measurement of solubilities in supercritical CO2 using high-pressure fiber-optic cells. Anal. Chem. 70, 2421-2425. https://doi.org/10.1021/ac971077h.

Connors, K.A., 1990. Chemical kinetics: the study of reaction rates in solution. Wiley-VCH Verlag GmbH.

Covaci, A., Harrad, S., Abdallah, M.A., Ali, N., Law, R.J., Herzke, D., de Wit, C.A., 2011. Novel brominated flame retardants: a review of their analysis, environmental fate and behaviour. Environ. Int. 37, 532-556. https://doi.org/10.1016/j.envint.2010.11.007.

389 Crank, J., 1979. The mathematics of diffusion. Oxford university press.
390 Cristale, J., Belé, T.G.A., Lacorte, S., de Marchi, M.R.R., 2019. Occurrence of flame retardants in landfills: A case
391 study in Brazil. Environ. Res. 168, 420-427. https://doi.org/10.1016/j.envres.2018.10.010.
392 Elektorowicz, M., El-Sadi, H., Lin, J., Ayadat, T., 2007. Effect of supercritical fluid extraction parameters and
393 clay properties on the efficiency of phenanthrene extraction. J. Colloid Interface Sci. 309, 445-452.
394 https://doi.org/10.1016/j.jcis.2006.12.038.
395 Freegard, K., Tan, G., Morton, R., 2006. Develop a Process to Separate Brominated Flame Retardants from WEEE
396 Polymers–Final report. Waste & Resources Action Programme (WRAP).
397 Fulton, J.L., Yee, G.G., Smith, R.D., 1993. Hydrogen Bonding of Simple Alcohols in Supercritical Fluids: An
398 FTIR Study. Supercritical Fluid Engineering Science. ACS Publications. https://doi.org/10.1021/bk-1992-
399 0514.ch014.
400 Gamse, T., Steinkellner, F., Marr, R., Alessi, P., Kikic, I., 2000. Solubility studies of organic flame retardants in
401 supercritical CO2. Ind. Eng. Chem. Res. 39, 4888-4890. https://doi.org/10.1021/ie000231e.
402 Georlette, P., 2001. New brominated flame retardants meet requirements for technical plastics. Plastics, Additives
403 and Compounding 3, 28-33. https://doi.org/10.1016/S1464-391X(01)80134-3.
404 Gill, R., Hurley, S., Brown, R., Tarrant, D., Dhaliwal, J., Sarala, R., Park, J.-S., Patton, S., Petreas, M., 2020.
405 Polybrominated diphenyl ether and organophosphate flame retardants in Canadian Fire Station Dust.
406 Chemosphere, 126669. https://doi.org/10.1016/j.chemosphere.2020.126669.
407 Gramatica, P., Cassani, S., Sangion, A., 2016. Are some “safer alternatives” hazardous as PBTs? The case study
408 of new flame retardants. J. Hazard. Mater. 306, 237-246. https://doi.org/10.1016/j.jhazmat.2015.12.017.
409 Grosso, C., Coelho, J., Pessoa, F., Fareleira, J., Barroso, J., Urieta, J., Palavra, A., Sovova, H., 2010. Mathematical
410 modelling of supercritical CO2 extraction of volatile oils from aromatic plants. Chem. Eng. Sci. 65, 3579-3590.
411 https://doi.org/10.1016/j.ces.2010.02.046.
412 Hahladakis, J.N., Velis, C.A., Weber, R., Iacovidou, E., Purnell, P., 2018. An overview of chemical additives
413 present in plastics: migration, release, fate and environmental impact during their use, disposal and recycling. J.
414 Hazard. Mater. 344, 179-199. https://doi.org/10.1016/j.jhazmat.2017.10.014.
415 Hojnik, M., Škerget, M., Knez, Ž., 2008. Extraction of lutein from Marigold flower petals–Experimental kinetics
416 and modelling. LWT-Food SCI. Technol 41. https://doi.org/10.1016/j.lwt.2007.11.017.
417 Huang, Z., Shi, X.-h., Jiang, W.-j., 2012. Theoretical models for supercritical fluid extraction. J. Chromatogr. A
418 1250, 2-26. https://doi.org/10.1016/j.chroma.2012.04.032.

IUPAC, 1997. Compendium of chemical terminology. Blackwell Scientific Publications Oxford. https://doi.org/10.1351/goldbook.B00626.

Jackson, K., Bowman, L.E., Fulton, J.L., 1995. Water solubility measurements in supercritical fluids and high-pressure liquids using near-infrared spectroscopy. Anal. Chem. 67, 2368-2372. https://doi.org/10.1021/ac00110a007.

Jokić, S., Velić, D., Bilić, M., BuCić-koJić, A., PlANiNić, M., ToMAS, S., 2010. Modelling of solid-liquid extraction process of total polyphenols from soybeans. Czech Journal of Food Sciences 28, 206-212. https://doi.org/10.17221/200/2009-CJFS.

Kayathi, A., Chakrabarti, P.P., Rocha, L.B., Cardozo-Filho, L., Jegatheesan, V., 2020. Selective Extraction of Polar Lipids of Mango kernel using Supercritical Carbon dioxide (SC-CO2) Extraction: Process Optimization of Extract Yield/Phosphorous content and Economic Evaluation. Chemosphere, 127639. https://doi.org/10.1016/j.chemosphere.2020.127639.

Khaled, A., Richard, C., Rivaton, A., Jaber, F., Sleiman, M., 2018. Photodegradation of brominated flame retardants in polystyrene: Quantum yields, products and influencing factors. Chemosphere 211, 943-951. https://doi.org/10.1016/j.chemosphere.2018.07.147.

Kim, Y.R., Harden, F.A., Toms, L.-M.L., Norman, R.E., 2014. Health consequences of exposure to brominated flame retardants: a systematic review. Chemosphere 106, 1-19. https://doi.org/10.1016/j.chemosphere.2013.12.064.

Kokoric, V., Theisen, J., Wilk, A., Penisson, C., Bernard, G., Mizaikoff, B., Gabriel, J.-C.P., 2018. Determining the Partial Pressure of Volatile Components via Substrate-Integrated Hollow Waveguide Infrared Spectroscopy with Integrated Microfluidics. Anal. Chem. 90, 4445-4451. https://doi.org/10.1021/acs.analchem.7b04425.

Laintz, K.E., Wai, C.M., Yonker, C.R., Smith, R.D., 1991. Solubility of fluorinated metal diethyldithiocarbamates in Supercritical carbon dioxide. J. Supercrit. Fluids 4, 194-198. https://doi.org/10.1016/0896-8446(91)90008-T.

Liu, K., Li, J., Yan, S., Zhang, W., Li, Y., Han, D., 2016. A review of status of tetrabromobisphenol A (TBBPA) in China. Chemosphere 148, 8-20. https://doi.org/10.1016/j.chemosphere.2016.01.023.

Lörchner, D., Kraus, W., Köppen, R., 2019. Photodegradation of the novel brominated flame retardant 2, 4, 6-Tris-(2, 4, 6-tribromophenoxy)-1, 3, 5-triazine in solvent system: Kinetics, photolysis products and pathway. Chemosphere 229, 77-85. https://doi.org/10.1016/j.chemosphere.2019.04.184.

Lu, J., Han, B., Yan, H., 1999. UV-Vis spectroscopic studies of solute–solvent and solute–cosolvent interactions in supercritical carbon dioxide. Phys. Chem. Chem. Phys. 1, 3269-3276. https://doi.org/10.1039/A901854I.

449 Ma, C., Yu, J., Wang, B., Song, Z., Xiang, J., Hu, S., Su, S., Sun, L., 2016. Chemical recycling of brominated
450 flame retarded plastics from e-waste for clean fuels production: a review. Renewable and Sustainable Energy
451 Reviews 61, 433-450. https://doi.org/10.1016/j.rser.2016.04.020.
452 Madras, G., Thibaud, C., Erkey, C., Akgerman, A., 1994. Modeling of supercritical extraction of organics from
453 solid matrices. AlChE J. 40, 777-785. https://doi.org/10.1002/aic.690400505.
454 Marioth, E., Bunte, G., Hardle, T., 1996. Supercritical fluid extraction of ABS-composites in order to separate
455 organic flame retardants. Polymer Recycling(UK) 2, 303-308.
456 Maurice, A., Theisen, J., Gabriel, J.-C.P., 2020. Microfluidic Lab-on-Chip Advances for Liquid-Liquid Extraction
457 Process Studies. Curr. Opin. Colloid Interface Sci. https://doi.org/10.1016/j.cocis.2020.03.001.
458 Nakajima, K., Kawakami, T., Ueno, T., Onishi, H., 2002. Method for treating thermoplastic resin composition
459 containing flame retardant. U. S. Patent, United States.
460 Ni, M., Xiao, H., Chi, Y., Yan, J., Buekens, A., Jin, Y., Lu, S., 2012. Combustion and inorganic bromine emission
461 of waste printed circuit boards in a high temperature furnace. Waste Manage. 32, 568-574.
462 https://doi.org/10.1016/j.wasman.2011.10.016.
463 Nimet, G., Da Silva, E.A., Palú, F., Dariva, C., dos Santos Freitas, L., Neto, A.M., Cardozo Filho, L., 2011.
464 Extraction of sunflower (Heliantus annuus L.) oil with supercritical CO2 and subcritical propane: Experimental
465 and modeling. Chem. Eng. J. 168, 262-268. https://doi.org/10.1016/j.cej.2010.12.088.
466 Peng, S., Liang, S., Yu, M., Li, X., 2014. Extraction of polybrominated diphenyl ethers contained in waste high
467 impact polystyrene by supercritical carbon dioxide. J. Mater. Cycles Waste Manage. 16, 178-185.
468 https://doi.org/10.1007/s10163-013-0169-y.
469 Poliakoff, M., Howdle, S.M., Kazarian, S.G., 1995. Vibrational spectroscopy in supercritical fluids: from analysis
470 and hydrogen bonding to polymers and synthesis. Angewandte Chemie International Edition in English 34, 1275-
471 1295. https://doi.org/10.1002/anie.199512751.
472 Sakai, S.-i., Watanabe, J., Honda, Y., Takatsuki, H., Aoki, I., Futamatsu, M., Shiozaki, K., 2001. Combustion of
473 brominated flame retardants and behavior of its byproducts. Chemosphere 42, 519-531.
474 https://doi.org/10.1016/S0045-6535(00)00224-1.
475 Sikorski, M.E., 1993. Recycling of polymeric materials from carpets and other multi-component structures by
476 means of supercritical fluid extraction. U. S. Patent, United States.
477 Sodeifian, G., Ghorbandoost, S., Sajadian, S.A., Ardestani, N.S., 2016. Extraction of oil from Pistacia khinjuk
478 using supercritical carbon dioxide: Experimental and modeling. J. Supecrit. Fluids 110, 265-274.

https://doi.org/10.1016/j.supflu.2015.12.004.

Sovová, H., 1994. Rate of the vegetable oil extraction with supercritical CO2—I. Modelling of extraction curves. Chem. Eng. Sci. 49, 409-414. https://doi.org/10.1016/0009-2509(94)87012-8.

Srinivasan, M., Smith, J., McCoy, B., 1990. Supercritical fluid desorption from activated carbon. Chem. Eng. Sci. 45, 1885-1895. https://doi.org/10.1016/0009-2509(90)87064-Y.

Stubbings, W.A., Nguyen, L.V., Romanak, K., Jantunen, L., Melymuk, L., Arrandale, V., Diamond, M.L., Venier, M., 2019. Flame retardants and plasticizers in a Canadian waste electrical and electronic equipment (WEEE) dismantling facility. Sci. Total Environ. 675, 594-603. https://doi.org/10.1016/j.scitotenv.2019.04.265.

Subra, P., Castellani, S., Jestin, P., Aoufi, A., 1998. Extraction of β-carotene with supercritical fluids: experiments and modelling. J. Supecrit. Fluids 12, 261-269. https://doi.org/10.1016/S0896-8446(98)00085-0.

Sunarso, J., Ismadji, S., 2009. Decontamination of hazardous substances from solid matrices and liquids using supercritical fluids extraction: A review. J. Hazard. Mater. 161, 1-20. https://doi.org/10.1016/j.jhazmat.2008.03.069.

Suzuki, M., Nakajima, K., Onishi, H., 2002. Method for treating flame retardant resin composition. U. S. Patent, United States.

Tan, C.S., Liou, D.C., 1989. Modeling of desorption at supercritical conditions. AlChE J. 35, 1029-1031. https://doi.org/10.1002/aic.690350616.

Taylor, L.T., 1996. Supercritical fluid extraction. Wiley New York.

Villanueva-Bermejo, D., Fornari, T., Calvo, M.V., Fontecha, J., Coelho, J.A., Filipe, R.M., Stateva, R.P., 2020. Application of a novel approach to modelling the supercritical extraction kinetics of oil from two sets of chia seeds. J. Ind. Eng. Chem. 82, 317-323. https://doi.org/10.1016/j.jiec.2019.10.029.

Wang, H., Hirahara, M., Goto, M., Hirose, T., 2004. Extraction of flame retardants from electronic printed circuit board by supercritical carbon dioxide. J. Supecrit. Fluids 29, 251-256. https://doi.org/10.1016/S0896-8446(03)00073-1.

Wang, Z., Zhou, Q., Guo, H., Yang, P., Lu, W., 2018. Determination of water solubility in supercritical CO2 from 313.15 to 473.15 K and from 10 to 50 MPa by in-situ quantitative Raman spectroscopy. Fluid Phase Equilib. 476, 170-178. https://doi.org/10.1016/j.fluid.2018.08.006.

Xiong, P., Yan, X., Zhu, Q., Qu, G., Shi, J., Liao, C., Jiang, G., 2019. A review of environmental occurrence, fate, and toxicity of novel brominated flame retardants. Environ. Sci. Technol. 53, 13551-13569. https://doi.org/10.1021/acs.est.9b03159.

509 Yu, G., Bu, Q., Cao, Z., Du, X., Xia, J., Wu, M., Huang, J., 2016. Brominated flame retardants (BFRs): a review
510 on environmental contamination in China. Chemosphere 150, 479-490.
511 https://doi.org/10.1016/j.chemosphere.2015.12.034.
512 Zhan, L., Zhao, X., Ahmad, Z., Xu, Z., 2020. Leaching behavior of Sb and Br from E-waste flame retardant
513 plastics. Chemosphere 245, 125684. https://doi.org/10.1016/j.chemosphere.2019.125684.
514 Zhang, C.C., Zhang, F.S., 2012. Removal of brominated flame retardant from electrical and electronic waste
515 plastic by solvothermal technique. J. Hazard. Mater. 221, 193-198. https://doi.org/10.1016/j.jhazmat.2012.04.033.
516 Zhao, Y.-B., Lv, X.-D., Ni, H.-G., 2018. Solvent-based separation and recycling of waste plastics: A review.
517 Chemosphere 209, 707-720. https://doi.org/10.1016/j.chemosphere.2018.06.095.
518 Zhou, X., Guo, J., Lin, K., Huang, K., Deng, J., 2013. Leaching characteristics of heavy metals and brominated
519 flame retardants from waste printed circuit boards. J. Hazard. Mater. 246-247, 96-102.
520 https://doi.org/10.1016/j.jhazmat.2012.11.065.
521 Zuiderveen, E., Slootweg, J.C., de Boer, J., 2020. Novel brominated flame retardants-A review of their occurrence
522 in indoor air, dust, consumer goods and food. Chemosphere, 126816.
523 https://doi.org/10.1016/j.chemosphere.2020.126816.